specific reaction of sheep sera during the detection of antibodies to the virus by enzyme-linked immunosorbent assay (ELISA).

In order to overcome these problems, we developed an ELISA using recombinant nucleoprotein of Crimean-Congo hemorrhagic fever virus and an indirect immunofluorescence assay using HeLa cells expressing the recombinant nucleoprotein for the detection of immunoglobulin G (IgG) to the virus in sheep sera. We describe an effective Crimean-Congo hemorrhagic fever virus antibody detection system for use with sheep sera using the recombinant nucleoprotein.

2. Materials and methods

2.1. Sera

Eighty sera samples collected from sheep in the western region of the Xinjiang Uygur Autonomous Region, PR China, were used. The region is known to be an endemic area of Crimean-Congo hemorrhagic fever (Yen et al., 1985). Thirty-nine sera samples collected from sheep in Shandong province (the disease-free area), one of the eastern provinces in PR China, were used as a control. These sera were collected in 2001 and used for the evaluation of the recombinant nucleoprotein-based antibody detection systems. The sera collected in the Xinjiang Uygur Autonomous Region and Shandong province were designated as Xinjiang sera and Shandong sera, respectively.

Fifty and 51 sera samples collected from sheep in the Xizang Autonomous Region (Tibet), a mountainous region, and Hainan province, an island province in southern China, respectively, were also used. These sera were collected in 1998 and were stored at −30 °C until use. The sera collected in the Xizang Autonomous Region and Hainan province were designated as Xizang sera and Hainan sera, respectively.

2.2. Expression of recombinant nucleoprotein of Crimean-Congo hemorrhagic fever virus

The recombinant nucleoprotein of the virus was expressed in insect cells with a recombinant baculovirus. The recombinant baculovirus, which expressed a full-length nucleoprotein of Crimean-Congo hemorrhagic fever virus tagged with 6 × histidine on the N-terminus, was generated as reported previously (Saijo et al., 2002a). The His-tagged recombinant nucleoprotein was expressed in insect cells by infection with the recombinant baculovirus and then purified (Saijo et al., 2002a). The negative control antigen was also prepared in the same way as described previously (Saijo et al., 2002a).

The HeLa cell line continuously expressing recombinant nucleoprotein of the virus was established as reported previously (Saijo et al., 2002b).

2.3. Indirect immunofluorescence assay

The details of the indirect immunofluorescence assays performed in the study were reported previously (Saijo et al., 2002b). The authentic antigens [Vero E6 cells infected with Crimean-Congo hemorrhagic fever (Chinese isolate 66019)] and the recombinant antigens (HeLa cells expressing the recombinant nucleoprotein) as well as the negative control antigens were prepared in the same way as reported previously (Saijo et al., 2002b). For the authentic antigens and recombinant antigens, non-infected Vero E6 cells and HeLa cells were used as control antigens. The authentic antigen- and recombinant antigen-positive slides were designated as authentic antigen-slides and recombinant antigen-slides, respectively. The authentic virus antigens were made in a high containment laboratory according to the regulations of the Institute of Epidemiology and Microbiology, Chinese Academy of Preventive Medicine, PR China.

Sheep serum samples were diluted at a dilution of 1:50 and placed on the authentic antigen-slides, recombinant antigen-slides and respective control slides. These slides were incubated under humidified conditions at 37 °C for 1 h. After washing with PBS, the antigens were reacted with fluorescein isothiocyanate (FITC)-conjugated rabbit *anti*-sheep IgG antibody (Vector Laboratories, Inc., Burlingame, CA) at a dilution of 1:70. Following another round of washing with PBS, the slides were examined for a staining pattern under a fluorescent microscope (Olympus, Tokyo, Japan) with an appropriate barrier and excitation filters for FITC visualization. The antibody-positive and -negative controls were included in each assay.

2.4. Enzyme-linked imunosorbent assay

ELISA was carried out as described previously except for the secondary antibody, the blocking reagents and washing solution (Saijo et al., 2002a). The blocking and the washing solutions were prepared according to the method used by Meegan et al. (1987). The blocking solution was composed of PBS containing 0.5% Tween-20, 500 μg dextran sulfate/ml and 5% heat-inactivated horse serum (Life Technologies) and the washing solution was composed of PBS containing 0.25% Tween-20 (Meegan et al., 1987). Briefly, half of the wells of the ELISA plates (PRO-BIND™, 96 well, flat bottom, Becton Dickinson Labware, Franklin Lakes, NJ) were coated with the predetermined optimal quantity of the purified recombinant nucleoprotein (approximately 100 ng/well) and the rest were coated with the negative control antigen at 4 °C overnight. After coat-

ing the plate with the antigen, each well of the plates was inoculated with 200 μl of the blocking solution and incubated for 1 h. After washing the plates three times with the washing solution, the antigen-coated and negative control antigen-coated wells were inoculated with the test samples (100 μl/well), which were 400 times diluted with the blocking solution. After a 1-h incubation period, the plates were washed three times with the washing solution. Then, each well of the plates was inoculated with a rabbit *anti*-sheep IgG antibody labeled with HRPO (1:1000-dilution; Zymed Laboratories, San Francisco, CA). After a further 1-h incubation period, the plates were washed and 100 μl of ABTS solution (Roche Diagnositics, Mannheim, Germany) was added to each well. The plates were incubated for 30 min at 37 °C and optical density (OD) was measured at 405 nm with a reference at 490 nm. The adjusted OD was calculated by subtracting the OD of the non-coated wells from that of the corresponding wells.

2.5. Statistical methods

Sensitivity, specificity and predictive values for positive and negative tests were calculated by standard methods (Griner et al., 1981). Sensitivity and specificity were defined as the probability that the target assay result was positive when the immunofluorescence assay using authentic antigen-slides showed a positive result and the probability that the target assay result was negative when the immunofluorescence assay showed negative result, respectively. The positive and negative predictive values were defined as the probability that the immunofluorescence assay using the authentic antigen-slides showed a positive reaction when the target assay was positive and the probability that the immunofluorescence assay showed a negative reaction when the target assay was negative.

Receiver operating characteristics (ROC) and two-graph-ROC (TG-ROC) curves were analyzed using Stat Flex ver. 5 software (Artech Co. Ltd., Osaka, Japan).

3. Results

3.1. Detection of antibodies to Crimean-Congo hemorrhagic fever virus by recombinant nucleoprotein-based indirect immunofluorescence assay

The staining patterns of the recombinant nucleoprotein expressed in HeLa cells and the authentic antigens in Vero E6 cells incubated with a sheep serum sample containing IgG antibodies to the virus are shown in Fig. 1. The staining patterns of the recombinant nucleoprotein in HeLa cells were granular, as were those of the Crimean-Congo hemorrhagic fever virus-infected Vero E6 cells.

Forty-nine of the 80 Xinjiang sera showed an antibody-positive reaction at a dilution of 1:50 and the rest showed a negative reaction in the authentic virus antigen-based indirect immunofluorescence assay. Forty-six of the 49 antibody-positive Xinjiang sera also showed a positive reaction in the immunofluorescence assay using the recombinant antigen-slides. On the other hand, two of the 31 antibody-negative Xinjiang sera showed a positive reaction in the recombinant nucleoprotein-based immunofluorescence assay. The Shandong sera were confirmed to be negative by both assays. All the data are summarized in Table 1. The sensitivity and specificity of the recombinant nucleoprotein-based indirect immunofluorescence assay were calculated as 94 and 97%, respectively. Both the positive and negative predictive values were calculated as 96%.

3.2. Detection of antibodies to Crimean-Congo hemorrhagic fever virus by recombinant nucleoprotein-based IgG ELISA

IgG antibodies to the virus was detected by the recombinant nucleoprotein-based IgG ELISA. The OD_{405} of each serum sample at a dilution of 1:400 is plotted in Fig. 2. ROC and TG-ROC curves are shown in Fig. 3. The area under the curve in ROC is 0.994 (Fig. 3a). If the cut-off is defined as the value at which sensitivity and specificity were equal (intersection point of the sensitivity curve and specificity curve), the cut-off value would be approximately 1.4 and sensitivity and specificity would be 95%. If the cut-off is defined as an OD_{405} of 1.8, the sensitivity would decrease to 90% but specificity would increase to 100% (Fig. 3a). In the case of a cut-off value of 1.8, 45 of the 49 antibody-positive Xinjiang sera would be confirmed as antibody-positive by the recombinant nucleoprotein-based IgG ELISA. The rest of the Xinjiang sera and all the Shandong sera showed a negative reaction in the IgG ELISA. The sensitivity and specificity were calculated as 92 and 100%, respectively.

3.3. Seroepidemiology

While 46 of the 80 Xinjiang sera showed a positive reaction in the indirect immunofluorescence assay using the recombinant antigen-slides, none of the Shangong, Xizang or Hainan sera were positive.

4. Discussion

The efficacy of the IgG ELISA using the recombinant nucleoprotein in detecting the IgG antibody to Crimean-Congo hemorrhagic fever virus has been reported previously for human serum samples (Marriott et al., 1994; Saijo et al., 2002a). A skim milk-based blocking

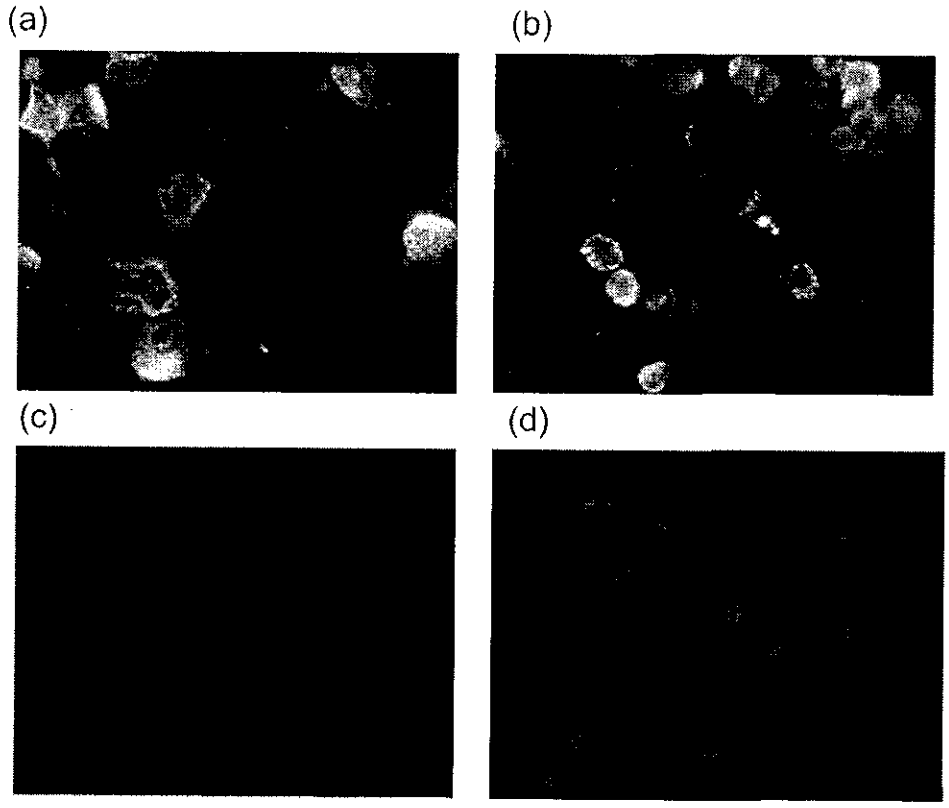

Fig. 1. Positive immunofluorescence staining of recombinant nucleoprotein-expressing HeLa cells (a) and Crimean-Congo hemorrhagic fever virus-infected Vero E6 cells (b) with a CCHFV antibody-positive sheep serum at a dilution of 1:50. The respective negative control cells, HeLa cells (c) and Vero cells (d) stained with the same serum are also shown.

Table 1
Relationship of the results between the authentic virus antigen-based and recombinant nucleoprotein-based indirect immunofluorescent assays

		Authentic antigen-assay ($N = 119$)	
		Positive	Negative
Recombinant antigen-assay	Positive	46	2
	Negative	3	68

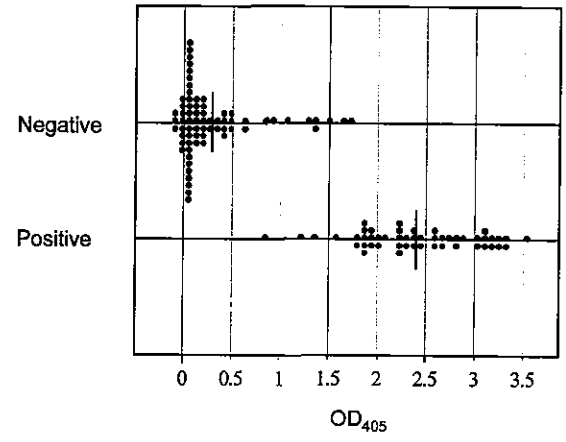

Fig. 2. Distribution of OD_{405} values obtained by the recombinant nucleoprotein-based IgG ELISA among the Crimean-Congo hemorrhagic fever virus antibody-positive and -negative serum samples as determined by the authentic virus antigen-based indirect immunofluorescence assay.

reagent was used in the IgG ELISA for human serum samples (Saijo et al., 2002a). However, we could not detect the specific antibody to the virus in this ELISA with high sensitivity and specificity because of a very strong non-specific reaction (data not shown). Therefore, we evaluated the IgG ELISA with a horse serum-based blocking solution containing dextran sulfate and Tween-20 and a washing solution containing a higher concentration of Tween-20 (0.25%). The non-specific reaction could be successfully reduced by these modifications.

The antibody-positive rates for Crimean-Congo hemorrhagic fever virus among the Xinjiang sera as determined by the authentic virus antigen-based indirect immunofluorescence assay, by the recombinant nucleoprotein-based indirect immunofluorescence assay and by the IgG ELISA were 61, 56 and 56%, respectively. It was found that there was no evidence of Crimean-Congo hemorrhagic fever virus infections in sheep in Shandong, Xiznag or Hainan, while approximately half of the sheep in Xinjiang were infected with CCHFV.

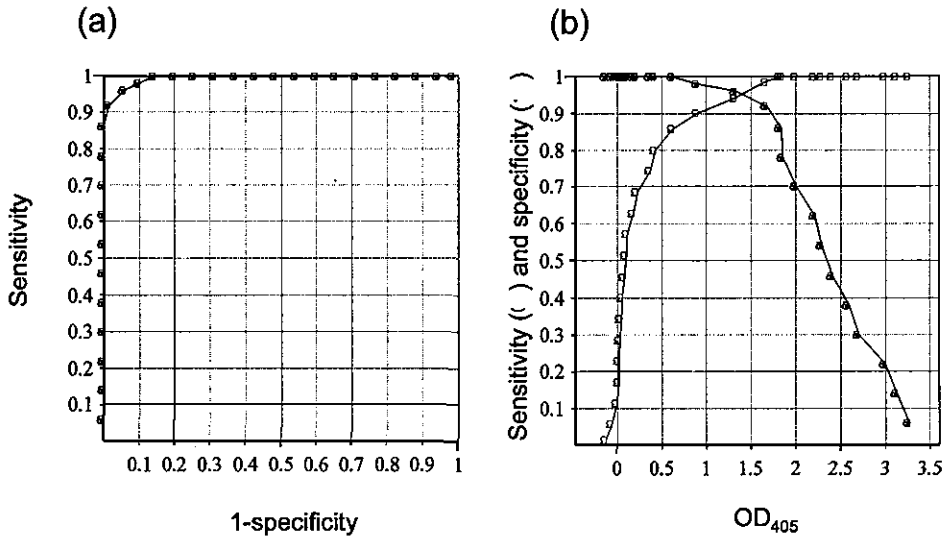

Fig. 3. ROC (a) and TG-ROC (b) analyses of the recombinant nucleoprotein-based IgG ELISA.

The highest OD_{405} value among the Shandong sera samples was 0.901. Seven sera showed higher values than this value in the sera found to be Crimean-Congo hemorrhagic fever virus antibody negative by the IgG ELISA (Fig. 2). These 7 sera were all from the Xinjiang area. Some of these 7 Xinjiang sera were considered to be virus antibody positive. If the cut-off value were defined 0.901, the positive predictive value of the IgG ELISA was calculated as 87%. This indicates that the 7 Xinjiang sera were Crimean-Congo hemorrhagic fever virus antibody positive with an 87% of probability.

Various methods including ELISA, indirect immunofluorescence assays, complement fixation methods, and reversed passive hemagglutination and inhibition methods have been used for detecting antibodies to Crimean-Congo hemorrhagic fever virus in sheep sera (Burt et al., 1993; Khan et al., 1997; Morrill et al., 1990; Saidi et al., 1975; Swanepoel et al., 1983a,b; Williams et al., 2000). Nevertheless, all these methods require the handling of the live virus at some stage, necessitating the use of a high security containment laboratory. The efficacy of the recombinant nucleoprotein as an antigen for IgG ELISA and immunofluorescence assay has been reported for human sera (Marriott et al., 1994; Saijo et al., 2002a,b), but not for sheep sera. In the present study, we demonstrate that the recombinant nucleoprotein is also a useful antigen for IgG ELISA and indirect immunofluorescence assay techniques for sheep sera. Unfortunately, outbreaks of Crimean-Congo hemorrhagic fever occur in areas so remote that insufficient sheep sera samples could be collected. Therefore, it is necessary to evaluate the recombinant nucleoprotein-based antibody detection systems for Crimean-Congo hemorrhagic fever virus using more serum samples to confirm the efficacy.

In summary, recombinant nucleoprotein-based antibody detection systems were developed for Crimean-Congo hemorrhagic fever virus. We believe that these systems may be of use in facilitating the epidemiological study of Crimean-Congo hemorrhagic fever infections.

Acknowledgements

We would like to thank Dr. B. Shimayi, Bachu County Center for Disease Prevention and Control, for his excellent assistance with this work. We would like to thank Ms X. Zhao and Ms X. Tao, Second Division of Viral Hemorrhagic Fever, Institute of Epidemiology and Microbiology, Chinese Academy of Preventive Medicine, for their excellent technical assistance with this work. We also thank Ms M. Ogata, Department of Virology 1, National Institute of Infectious Diseases, Tokyo, Japan, for her technical and official assistance. This work was supported by a Grant-in-Aid from the Ministry of Health, Labor and Welfare of Japan, from Japan Food Hygiene Association, Tokyo, Japan.

References

Burt, F.J., Swanepoel, R., Braack, L.E.O., 1993. Enzyme-linked immunosorbent assays for the detection of antibody to Crimean-Congo haemorrhagic fever virus in the sera of livestock and wild vertebrates. Epidemiol. Infect. 111, 547–557.

Gonzalez-Scarano, F., Nathanson, N., 1996. Bunyaviridae. In: Fields, B., Knipe, D.M., Howley, P. (Eds.), Fields Virology, 3rd ed.. Lippincott-Reven, Philadelphia, pp. 1473–1504.

Griner, P.F., Mayewski, R.J., Mushlin, A.I., Greenland, P., 1981. Selection and interpretation of diagnostic tests and procedures. Principles and applications. Ann. Intern. Med. 94, 557–592.

Hoogstraal, H., 1979. The epidemiology of tick-borne Crimean-Congo hemorrhagic fever in Asia, Europe, and Africa (Review). J. Med. Entomol. 15, 307–417.

Khan, A.S., Maupin, G.O., Rollin, P.E., Noor, A.M., Shurie, H.H., Shalabi, A.G., Wasef, S., Haddad, Y.M., Sadek, R., Ijaz, K., Peters, C.J., Ksiazek, T.G., 1997. An outbreak of Crimean-Congo hemorrhagic fever in the United Arab Emirates, 1994–1995. Am. J. Trop. Med. Hyg. 57, 518–525.

Marriott, A.C., Polyzoni, T., Antoniadis, A., Nuttall, P.A., 1994. Detection of human antibodies to Crimean-Congo haemorrhagic fever virus using expressed viral nucleocapsid protein. J. Gen. Virol. 75, 2157–2161.

Meegan, J.M., Yedloutschnig, R.J., Peleg, B.A., Shy, J., Peters, C.J., Walker, J.S., Shope, R.E., 1987. Enzyme-linked immunosorbent assay for detection of antibodies to Rift Valley fever virus in ovine and bovine sera. Am. J. Vet. Res. 48, 1138–1141.

Morrill, J.C., Soliman, A.K., Iman, I.Z., Botros, B.A.M., Moussa, M.I., Watts, D.M., 1990. Serological evidence of Crimean-Congo haemorrhagic fever viral infection among camels imported into Egypt. J. Trop. Med. Hyg. 93, 201–204.

Saidi, S., Casals, J., Faghih, M.A., 1975. Crimean hemorrhagic fever-Congo (CHF-C) virus antibodies in man, and in domestic and small mammals, in Iran. Am. J. Trop. Med. Hyg. 24, 353–357.

Saijo, M., Tang, Q., Niikura, M., Maeda, A., Ikegami, T., Prehaud, C., Kurane, I., Morikawa, S., 2002a. Recombinant nucleoprotein based enzyme-linked immunosorbent assay for detection of immunoglobulin G to Crimean-Congo hemorrhagic fever virus. J. Clin. Microbiol. 40, 1587–1591.

Saijo, M., Tang, Q., Niikura, M., Maeda, A., Ikegami, T., Prehaud, C., Kurane, I., Morikawa, S., 2002b. An immunofluorescence technique for detection of immunoglobulin G antibodies to Crimean-Congo hemorrhagic fever virus using HeLa cells expressing recombinant nucleoprotein. J. Clin. Microbiol. 40, 372–375.

Swanepoel, R., Shepherd, A.J., Leman, P.A., Shepherd, S.P., 1985. A common-source outbreak of Crimean-Congo haemorrhagic fever on a dairy farm. S. Afr. Med. J. 68, 635–637.

Swanepoel, R., Struthers, J.K., McGillivary, G.M., 1983a. Reversed passive heamagglutination and inhibition with Rift Valley fever and Crimean-Congo hemorrhagic fever viruses. Am. J. Trop. Med. Hyg. 32, 610–617.

Swanepoel, R., Struthers, J.K., Shepherd, A.J., 1983b. Crimean-Congo hemorrhagic fever in South Africa. Am. J. Trop. Med. Hyg. 32, 1407–1415.

Williams, R.J., Ali-Busaidy, S., Mehta, F.R., Maupin, G.O., Wagoner, K.D., Ali-Awaidy, S., Suleiman, A.J.M., Khan, A.S., Peters, C.J., Ksiazek, T.G., 2000. Crimean-Congo haemorrhagic fever: a seroepidemiological and tick survey in the Sultanate of Oman. Trop. Med. Int. Health 5, 99–106.

Yen, Y.C., Kong, L.X., Lee, L., Zhang, Y.Q., Li, F., Cai, B.J., Gao, S.Y., 1985. Characteristics of Crimean-Congo hemorrhagic fever virus (Xinjiang strain) in China. Am. J. Trop. Med. Hyg. 34, 1179–1182.

CLINICAL AND DIAGNOSTIC LABORATORY IMMUNOLOGY, Jan. 2003, p. 83–87 Vol. 10, No. 1
1071-412X/03/$08.00+0 DOI: 10.1128/CDLI.10.1.83–87.2003

Analysis of Linear B-Cell Epitopes of the Nucleoprotein of Ebola Virus That Distinguish Ebola Virus Subtypes

Masahiro Niikura,[1]† Tetsuro Ikegami,[1,2] Masayuki Saijo,[1] Takeshi Kurata,[3] Ichiro Kurane,[1] and Shigeru Morikawa[1]*

Department of Virology[1] and Department of Pathology,[3] National Institute of Infectious Diseases, Tokyo 208-0011, and Department of Biomedical Science, Graduate School of Agricultural and Life Sciences, The University of Tokyo, Tokyo 113-8657,[2] Japan

Received 19 April 2002/Returned for modification 19 August 2002/Accepted 8 September 2002

Ebola virus consists of four genetically distinguishable subtypes. We developed monoclonal antibodies (MAbs) to the nucleoprotein (NP) of Ebola virus Zaire subtype and analyzed their cross-reactivities to the Reston and Sudan subtypes. We further determined the epitopes recognized by these MAbs. Three MAbs reacted with the three major subtypes and recognized a fragment containing 110 amino acids (aa) at the C-terminal extremity. They did not show specific reactivities to any 10-aa short peptides in Pepscan analyses, suggesting that these MAbs recognize conformational epitope(s) located within this region. Six MAbs recognized a fragment corresponding to aa 361 to 461 of the NP. Five of these six MAbs showed specific reactivities in Pepscan analyses, and the epitopes were identified in two regions, aa 424 to 430 and aa 451 to 455. Three MAbs that recognized the former epitope region cross-reacted with all three subtypes, and one that recognized the same epitope region was Zaire specific. One MAb, which recognized the latter epitope region, was reactive with Zaire and Sudan subtypes but not with the Reston subtype. These results suggest that Ebola virus NP has at least two linear epitope regions and that the recognition of the epitope by MAbs can vary even within the same epitope region. These MAbs showing different subtype specificities might be useful reagents for developing an immunological system to identify Ebola virus subtypes.

Ebola virus is a filamentous negative-strand RNA virus, which naturally infects humans and nonhuman primates. In these hosts, Ebola virus causes severe hemorrhagic fever with very high mortality (27, 28). Despite an extensive search, the natural reservoir of Ebola virus is not yet known (2, 10). Ebola virus consists of four genetically distinguishable subtypes: Zaire, Sudan, Côte d'Ivoire, and Reston (3). The former three cause severe hemorrhagic fever both in humans and nonhuman primates. Of them, the Zaire and Sudan subtypes have been the cause of major outbreaks (21, 26, 27, 29). The mortality in the infected patients varies depending on the subtype (1, 26, 29). Notably, the Reston subtype has infected humans on several occasions but with no associated clinical symptoms (12, 13, 17), whereas it caused severe hemorrhagic fever in nonhuman primates, especially in Macaca monkeys, like the other subtypes (4, 14). Therefore, it is important to distinguish between these subtypes and to elucidate the molecular basis for the differences.

Ebola virus contains seven structural proteins (16). Nucleoprotein (NP) is one of the most abundant structural proteins among the Ebola virus-encoded proteins (8) and consists of 739 (Zaire and Reston) or 738 (Sudan) amino acids (aa) (6, 20) (GenBank accession no. AF173836). The N-terminal half of the NP is highly hydrophobic and relatively conserved among subtypes, whereas the C-terminal half is variable. Cytotoxic T cells specific to aa 43 to 53 of NP have shown the potential to protect animals from experimental Ebola virus infection, although NP-specific antibodies failed to protect these animals (25).

Monoclonal antibodies (MAbs) specific to the glycoprotein (GP) of Ebola virus have been reported, and functional aspects of these MAbs were analyzed (7, 11, 23, 24). Several linear epitopes on GP molecules were also defined (24). However, considering its abundance and strong antigenicity, NP should be a better target for viral antigen detection. We have been developing MAbs to the NP of Ebola virus subtype Zaire for laboratory diagnostic purposes. We have already reported that an MAb that recognizes 26 aa near the C terminus is reactive with at least three subtypes of Ebola virus NP, and we applied this MAb to an antigen capture enzyme-linked immunosorbent assay (ELISA) (15). In the present study, we report MAbs that show different Ebola virus subtype specificities, and define linear epitopes on NP recognized by these MAbs.

MATERIALS AND METHODS

Cells. The P3/Ag568 myeloma cell line and all hybridomas were maintained in RPMI 1640 (Life Technologies, Rockville, Md.) supplemented with 10% fetal bovine serum and antibiotics (100 U of penicillin and 100 μg of streptomycin/ml; Life Technologies). HAT supplement (100 μM sodium hypoxanthine, 0.4 μM aminopterin, and 16 μM thymidine; Life Technologies) was added as necessary. Tn5 cells were maintained in TC100 (Life Technologies) supplemented with 5% tryptose phosphate broth (Difco, Detroit, Mich.), 10% fetal bovine serum, and kanamycin (60 μg/ml; Meiji Seika, Tokyo, Japan).

Recombinant proteins. The full-length recombinant NP (rNP) of Ebola virus Zaire subtype (Mayinga strain) was expressed in Tn5 cells with a histidine tag at the N-terminal end by using the recombinant baculovirus system and then purified as described previously (18). Partial peptides of Zaire NP were expressed with a glutathione *S*-transferase (GST) tag at the N-terminal end in bacteria by using a pGEX2T vector (Amersham Pharmacia, Little Chalfont, United Kingdom). The expressed fusion proteins were purified by using glutathione-agarose

* Corresponding author. Mailing address: 4-7-1 Gakuen, Musashimurayama, 208-0011 Tokyo, Japan. Phone: 81-42-561-0771, ext. 791. Fax: 81-42-561-2039. E-mail: morikawa@nih.go.jp.

† Present address: USDA-ARS Avian Disease and Oncology Laboratory, East Lansing, MI 48823.

TABLE 1. Summary of the MAb characteristics

MAb	Isotype	IFA result[d] with subtype:			Recognition result[d]		
		Zaire	Reston	Sudan	No. of fragments[a]	Peptide no.[b]	aa[c]
3-9E	G1	+	−	−	5	420–424	D_{424}DDIPF$_{429}$
3-3A	G2b	+	+	+	5	421–426	D_{426}IPFP$_{430}$
1-5D	G1	+	+	+	5	421–426	D_{426}IPFP$_{430}$
2-9D	G1	+	+	+	5	421–426	D_{426}IPFP$_{430}$
1-7C	G1	+	−	+	5 and 6	446–451	D_{451}TTIP$_{455}$
3-7D	G1	+	+	+	5		
3-3D	G1	+	+	+	8		
3-1E	G1	+	+	+	8		
1-9E	G3	+	+	+	8		
2-11G	G1	+	+	−	8		
2-11C	G1	+	+	+			

[a] That is, the number of GST-fused partial fragments that showed reactivity with each MAb in an ELISA.

[b] Peptide numbers reactive in the Pepscan analyses are shown as the first amino acid number of the representative amino acid sequence of the NP.

[c] The minimum amino acid sequence recognized by each MAb was deduced from the results of the Pepscan analyses. The positions of the amino acids in the NP sequence are in subscript.

[d] "+" indicates a positive reaction, and "−" indicates a negative reaction.

as described previously (18). NP-5, NP-6, NP-7, and NP-8 represent aa 361 to 461, aa 451 to 551, aa 541 to 640, and aa 630 to 739 (C-terminal end) of Zaire NP, respectively (18). For the comparison of reactivities among the subtypes, GST fusion peptides corresponding to aa 421 to 458 were expressed by pGEX2T in bacteria according to the amino acid sequences of Zaire (20), Reston (6), and Sudan (GenBank accession no. AF173836) subtypes, respectively.

Immunological assays. ELISA was performed as reported previously (18) with purified rNP or partial NP peptides as the antigen. Linear epitopes on the NP were determined by using Pepscan (Chiron Technologies, Clayton, Australia) according to the manufacturer's instructions. Briefly, 194 peptides were prepared as 14-aa biotinylated peptides, including a 4-aa spacer sequence (SGSG) at the N-terminal end, according to the amino acid sequence of the Zaire subtype. The peptides were shifted by 1 aa, with a consecutive overlap of 9 aa to cover the entire NP-5 (aa 361 to 461) and NP-8 (aa 630 to 739) fragments. Immunoplates were coated with streptoavidin and blocked by sodium casein. The biotinylated peptides were added to each well, and the bound peptides were examined for their reactivity to MAbs with horseradish peroxidase-labeled anti-mouse immunoglobulin G (IgG; H+L) conjugate (Zymed, San Francisco, Calif.) and ABTS [2,2'azinobis(3-ethylbenzthiazolinesulfonic acid)] substrate (Roche Diagnostics, Mannheim, Germany). The average and standard deviation (SD) of each MAb were calculated based on the optical density (OD) values for the entire peptide set representing either NP-5 or NP-8. The peptides that showed ODs above the average + 2 SDs were considered positive. The peptide whose neighboring two peptides were both positive was also considered positive. To determine subtype specificities, 14-aa biotinylated-peptides, including a 4-aa spacer sequence (SGSG) at the N-terminal end, corresponding to aa 421 to 430 and aa 449 to 458 were synthesized according to the amino acid sequences of the Reston, Sudan, and Zaire subtypes, respectively (Sawady Technology, Tokyo, Japan).

Immunoblot analyses were performed with a semidry apparatus by a standard method with nylon membranes (Millipore, Bedford, Mass.). Reacted MAbs were detected with the horseradish peroxidase-labeled anti-mouse IgG (H+L) conjugate and a POD immunostain set (Wako Pure Chemicals, Osaka, Japan). Indirect immunofluorescence assay (IFA) was done as previously described with HeLa cells stably expressing rNP derived from either the Zaire or the Reston subtype as the antigen (19). IFA with the Sudan subtype was performed with an IFA antigen provided by J. B. McCormick (then at the Centers for Disease Control and Prevention, Atlanta, Ga.) in 1987. This antigen consisted of Maleo strain-infected Vero E6 cells fixed in acetone after gamma irradiation. The cDNA encoding the NP of the Reston subtype was isolated from infected monkey specimens as previously described (6) and stably expressed in HeLa cells (6a).

MAbs. Hybridomas and MAbs were prepared as described previously (15). Briefly, BALB/c mice were immunized with purified rNP of the Zaire subtype that was expressed by using a baculovirus expression system. The spleen cells were fused with P3/Ag568 myeloma line cells, and hybridomas were established. The hybridomas were primarily screened by ELISA with purified rNP of the Zaire subtype. For IFA, either mouse ascitic fluids or culture supernatants of the hybridomas were used at a dilution of 1:100 or without dilution, respectively. For ELISA and immunoblotting, the ascitic fluids and culture supernatants were used at dilutions of 1:1,000 and 1:10, respectively. Isotypes of the MAbs were determined by using a mouse MAb isotyping kit (Life Technologies).

RESULTS

Subtype specificity of MAbs in IFA. Ebola virus subtype specificity of 11 IgG MAbs was examined by IFA. Although these MAbs were initially selected on the basis of their reactivity to the rNP of the Zaire subtype in ELISA, all were reactive in IFA, as well with HeLa cells expressing rNP of Zaire (Table 1). Eight MAbs reacted with all three subtypes. MAb 1-7C reacted with the Zaire and Sudan subtypes but not with the Reston. 2-11G reacted with the Zaire and Reston subtypes but not with the Sudan. 3-9E reacted only with the Zaire subtype. These results that suggest these MAbs recognize different antigenic epitopes on the NP.

Definition of the epitopes recognized by the MAbs. We attempted to elucidate the basis for the different patterns of specificity of these MAbs. The localization of epitopes was determined by ELISA with four partial overlapping fragments, NP-5 to NP-8, representing the C-terminal half of the NP (Fig. 1). Six clones recognized the NP-5 fragment, indicating that the

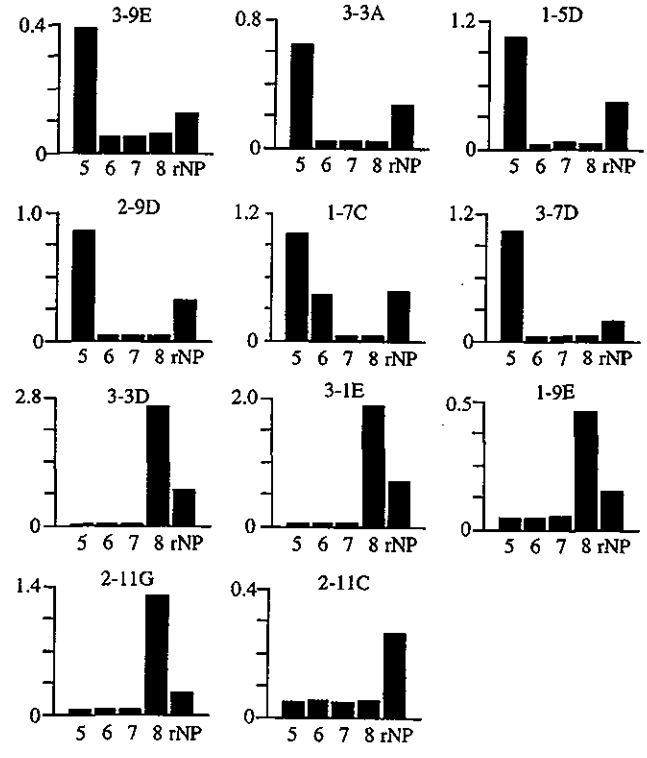

FIG. 1. Localization of antigenic epitopes on the NP. The reactivity of each MAb with GST-fused partial polypeptides of the NP (Zaire) was examined in ELISA. NP-5, NP-6, NP-7, and NP-8 (columns 5, 6, 7 and 8, respectively) represent aa 361 to 461, aa 451 to 551, aa 541 to 640, and aa 630 to 739 of the NP, respectively. As a positive control, rNP (entire open reading frame) expressed with a histidine tag was included. Results are expressed as absorbance at OD at 405 nm (OD_{405}).

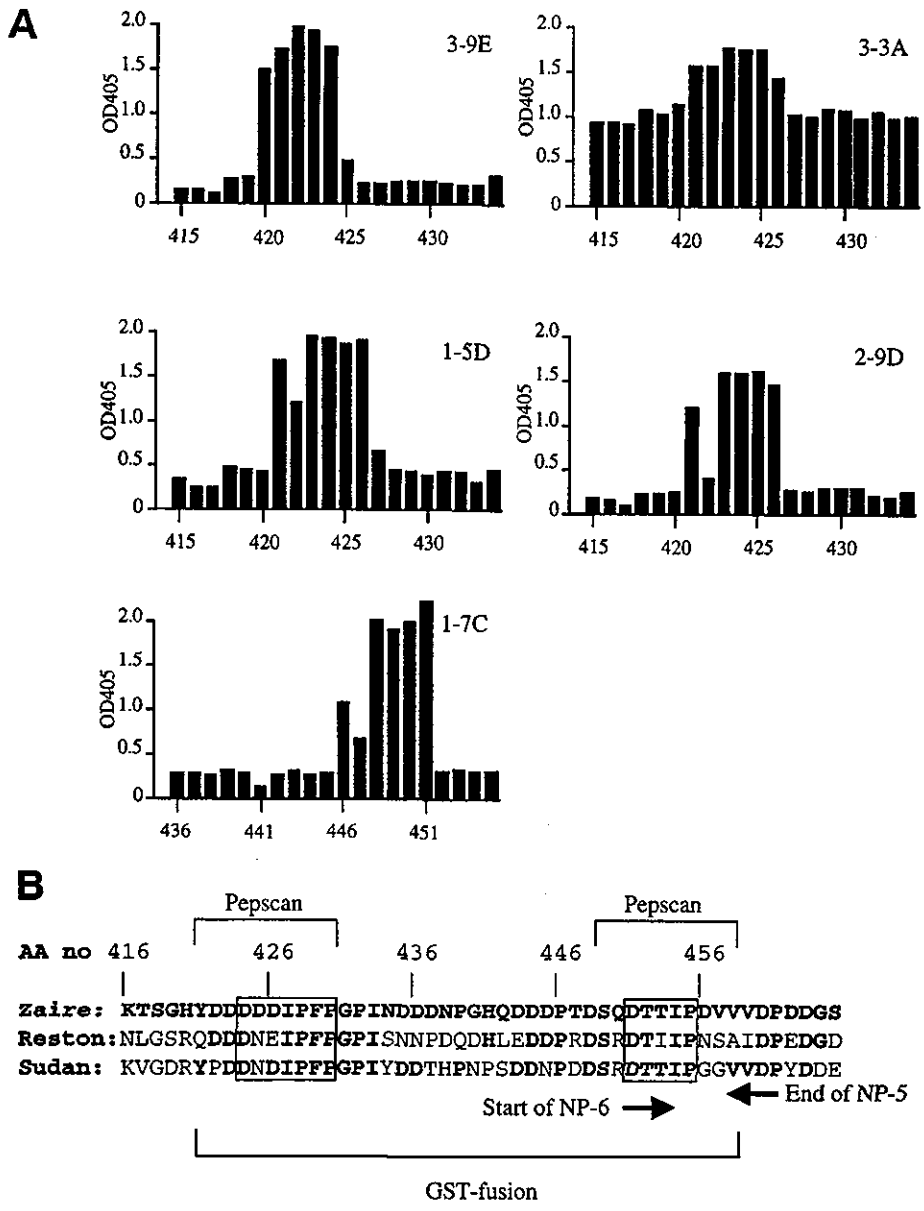

FIG. 2. (A) Pepscan analyses to determine the linear antigenic epitopes recognized by MAbs. Each overlapping peptide contains a 10-aa sequence of NP (Zaire) and is indicated by the position of the first amino acid. Results are expressed as absorbance at OD_{405}. The average absorbance values (SDs) for each MAb were as follows 0.31 (0.36), 1.07 (0.17), 0.43 (0.38), 0.28 (0.30), and 0.33 (0.38) for 3-9E, 3-3A, 1-5D, 2-9D, and 1-7C, respectively. (B) Amino acid sequences, including the linear epitope regions on the NP of three Ebola virus subtypes. The sequence of Zaire and the identical amino acid in the Reston and Sudan sequences are shown in boldface. Amino acid positions in the entire NP (AA no) are indicated above the sequence. The last and the first amino acid for NP-5 and NP-6, respectively, are indicated by arrows below the sequences. The regions used in the immunoblot assay (GST fusion) and ELISA (Pepscan) for comparison among subtypes are also indicated below and above the sequences, respectively. Epitope regions identified by Pepscan are boxed.

epitopes of these MAbs were located within aa 361 to 461. Among them, MAb 1-7C was reactive with both NP-6 and NP-5. Four MAbs recognized NP-8, indicating that they recognize amino acid sequences within the sequence from aa 630 to 739. 2-11C did not show specific reactivity with any of the partial fragments and was not characterized further.

To further localize the epitopes recognized by these 10 MAbs, Pepscan analyses were employed. Selected results are shown in Fig. 2A. No MAb specific to NP-8 (3-3D, 3-1E, 1-9E, and 2-11G) was reactive to any oligopeptides (data not shown), indicating that these MAbs recognize conformational epitope(s). Five of six MAbs specific to NP-5 showed reactivities in the Pepscan analysis. 3-9E reacted with 10-aa oligopeptides starting from aa 420, 421, 423, and 424 of the NP, indicating the recognition of the amino acid sequence of D_{424}DDIPF$_{429}$ (Fig. 2B). 3-3A, 1-5D, and 2-9D reacted with peptides starting from aa 421 through 426, indicating the recognition of D_{426}IPFP$_{430}$. 3-3A inherently showed higher background in this assay; yet it showed a unique positive spike at these peptides. 1-7C reacted with peptides starting from aa 446 through

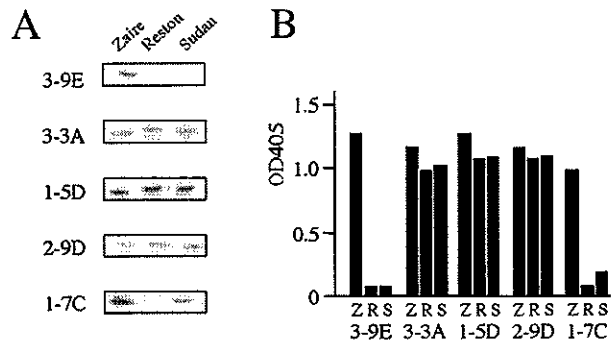

FIG. 3. (A) Reactivities of MAbs to Ebola virus subtypes in immunoblot assay. GST fusion polypeptides representing aa 421 to 458 of the NPs of Zaire, Reston, and Sudan subtypes were expressed in *E. coli*, and equal amounts were separated by sodium dodecyl sulfate-polyacrylamide gel electrophoresis. After samples were blotted to nylon membranes, the reactivity of the MAbs was examined. (B) Reactivities of MAbs to Ebola virus subtypes in ELISA. Oligopeptides containing the linear epitope regions (aa 421 to 430 and aa 449 to 458, respectively) of the NPs of Zaire (Z), Reston (R), and Sudan (S) subtypes were examined by ELISA. For 3-9E, 3-3A, 1-5D, and 2-9D, the oligopeptide representing aa 421 to 430 was used. For 1-7C, the oligopeptide representing aa 449 to 458 was used. The results are expressed as the absorbance at OD_{405}.

451, indicating the recognition of D_{451}TTIP$_{455}$, which is on both NP-5 and -6 (Fig. 2B). This agreed with the results that 1-7C was reactive to both NP-5 and -6 in ELISA. 3-7D failed to react with any of the 10-aa oligopeptides (data not shown).

Cross-reactivities of MAbs in immunoblotting and ELISA. We next examined the subtype specificities of these five epitope-mapped MAbs by other immunological methods. Reactivities in immunoblot analyses were examined by using GST fusion peptides representing the epitope regions (aa 421 to 458) of the Zaire, Reston, and Sudan subtypes (Fig. 2B and 3). 3-3A, 1-5D, and 2-9D were reactive with all three subtypes in the immunoblotting, as in IFA. 3-9E and 1-7C also showed the same reaction pattern in the immunoblotting as in IFA; 3-9E reacted with only the Zaire subtype, whereas 1-7C reacted with the Zaire and Sudan but not with the Reston subtype.

The recognition patterns among the three subtypes were further examined by ELISA by using 14-mer oligopeptides representing the epitope regions (Fig. 2B and 3B). 3-3A, 1-5D, and 2-9D showed reactivity to all three subtypes, as in the other two assays. 3-9E reacted only with the Zaire, whereas 1-7C reacted with both the Zaire and Sudan subtypes but not with the Reston subtype, as in IFA and immunoblotting. The reactivity of 1-7C with the Sudan subtype was, however, weaker than that with the Zaire subtype. These results indicate that 3-9E is Zaire specific and that 1-7C is cross-reactive for Zaire and Sudan subtypes, respectively. 3-3A, 1-5D, and 2-9D were cross-reactive for all three subtypes.

DISCUSSION

We have established MAbs to the NP of Ebola virus subtype Zaire. With these MAbs, two linear epitopes that seem useful for the differentiation of Ebola virus subtypes were identified. In fact, the NPs of the Zaire, Sudan and Reston subtypes of Ebola virus were successfully segregated by using combinations of these MAbs. Unfortunately, since sequence information or antigenic materials of the NP of the Côte d'Ivoire subtype was not available to us, we could not examine whether these MAbs were reactive to this subtype. Comparison of the GP sequences among Ebola virus subtypes indicated that the Côte d'Ivoire subtype was closer to Zaire than to Reston (3, 22). Although only a single case of confirmed human infection caused by subtype Côte d'Ivoire has been reported (5, 9), it is necessary to examine whether these MAbs may react with the NP of this subtype to further determine the usefulness of this panel of MAbs for subtype identification.

We determined that 9 of 10 MAbs recognized the C-terminal half of NP. The highly hydrophobic nature of the N-terminal half of NP (16) may be one of the reasons why most of the MAbs recognized the C-terminal half. In the C-terminal half, only NP-5 and NP-8, which span aa 361 to 461 and aa 630 to 739, respectively, were reactive with these MAbs. We identified two linear antigenic epitope regions on NP-5 by Pepscan analyses. None of the MAbs specific to NP-8 showed reactivity in the Pepscan analyses, suggesting that these MAbs recognize conformational epitope(s) formed by more than 10 aa or discontinuous ones. We have previously reported that one of these MAbs, 3-3D, recognized a nonlinear epitope formed by 26-aa residues spanning aa 648 to 673 (15). Considering that 2-11G failed to cross-react with the Sudan subtype in IFA whereas the others were reactive with all three subtypes, we assume that at least two different recognition sites exist on this C-terminal region.

One linear epitope region on NP-5 was located between aa 420 and 426. Recognition of this epitope region by MAbs varied both in the minimum amino acid requirement and the critical amino acid residue within the epitope. This diversity resulted in differences in subtype specificities and cross-reactivities of the MAbs (Fig. 2B). Three MAbs—3-3A, 1-5D, and 2-9D—recognized amino acid sequence of D_{426}IPFP$_{430}$ and cross-reacted with Reston, in which D_{426} was changed to E. This means the amino acid replacement from D_{426} to E_{426} was not crucial for recognition by these three MAbs. 3-9E recognized the amino acid sequence of D_{424}DDIPF$_{429}$ and reacted only with the Zaire subtype. This specificity may be attributed to the amino acid difference at position 425 that is D for Zaire but N for both Reston and Sudan subtypes.

The other linear epitope recognized by 1-7C was identified as D_{451}TTIP$_{455}$. This amino acid sequence is conserved between the Zaire and Sudan subtypes, whereas aa 453 is I in Reston (Fig. 2B). MAb 1-7C was reactive with Zaire and Sudan subtypes as expected, but it failed to recognize Reston subtype in all three assays. In ELISA, 1-7C showed lower OD values with the Sudan subtype than with the Zaire subtype. It is not clear whether this is due to a partial interference by the surrounding amino acid on the binding of the MAb to the NP or to that on the binding of the biotinylated peptide to streptavidin coated on the plate.

1-7C recognized an amino acid sequence conserved between the Zaire and Sudan subtypes and was reactive with these two subtypes in all three immunological assays but not reactive with Reston. 3-9E showed a Zaire-specific reaction in all three assays. Thus, these two MAbs, as well as others reactive with all three subtypes, are useful for discriminating the subtypes of Ebola virus.

ACKNOWLEDGMENTS

We gratefully acknowledge M. Ogata, Department of Virology 1, National Institute of Infectious Diseases.

This work was supported by grants from the Ministry of Health, Labor, and Welfare of Japan.

REFERENCES

1. **Baron, C. B., J. B. McCormick, and O. A. Zubeir.** 1983. Ebola virus disease in southern Sudan: hospital dissemination and intrafamilial spread. Bull. W. H. O. **61**:997–1003.
2. **Breman, J. G., K. M. Johnson, G. van der Groen, C. B. Robbins, M. V. Szczeniowski, K. Ruti, P. A. Webb, F. Meier, and D. L. Heymann.** 1999. A search for Ebola virus in animals in the Democratic Republic of the Congo and Cameroon: ecologic, virologic, and serologic surveys, 1979–1980. J. Infect. Dis. **179**(Suppl. 1):S139–S147.
3. **Feldmann, H., and M. P. Kiley.** 1999. Classification, structure, and replication of filovirus, p. 1–21. *In* H.-D. Klenk (ed.), Marburg and Ebola viruses. Springer-Verlag, Berlin, Germany.
4. **Fisher-Hoch, S. P., T. L. Brammer, S. G. Trappier, L. C. Hutwagner, B. B. Farrar, S. L. Ruo, B. G. Brown, L. M. Hermann, G. I. Perez-Oronoz, C. S. Goldsmith, M. A. Hanes, and J. B. McCormick.** 1992. Pathogenic potential of filoviruses: role of geographic origin of primate host and virus strain. J. Infect. Dis. **166**:753–763.
5. **Formenty, P., C. Boesch, M. Wyers, C. Steiner, F. Donati, F. Dind, F. Walker, and B. Le Guenno.** 1999. Ebola virus outbreak among wild chimpanzees living in a rain forest of Cote d'Ivoire. J. Infect. Dis. **179**(Suppl. 1): S120–S126.
6. **Ikegami, T., A. B. Calaor, M. E. Miranda, M. Niikura, M. Saijo, I. Kurane, Y. Yoshikawa, and S. Morikawa.** 2001. Genome structure of Ebola virus subtype Reston: differences among Ebola subtypes. Arch. Virol. **146**:2021–2027.

6a. **Ikegami, T., M. Saijo, M. Niikura, M. E. Miranda, A. B. Calaor, M. Hernandez, D. L. Manalo, I. Kurane, Y. Yoshikawa, and S. Morikawa.** 2002. Development of an immunofluorescence method for the detection of antibodies to Ebola virus subtype Reston by the use of recombinant nucleoprotein-expressing HeLa cells. Microbiol. Immunol. **46**:633–638.

7. **Ito, H., S. Watanabe, A. Takada, and Y. Kawaoka.** 2001. Ebola virus glycoprotein: proteolytic processing, acylation, cell tropism, and detection of neutralizing antibodies. J. Virol. **75**:1576–1580.
8. **Kiley, M. P., R. L. Regnery, and K. M. Johnson.** 1980. Ebola virus: identification of virion structural proteins. J. Gen. Virol. **49**:333–341.
9. **Le Guenno, B., P. Formentry, M. Wyers, P. Gounon, F. Walker, and C. Boesch.** 1995. Isolation and partial characterisation of a new strain of Ebola virus. Lancet **345**:1271–1274.
10. **Leirs, H., J. K. Mills, J. W. Krebs, J. E. Childs, D. Akaibe, N. Woollen, G. Ludwig, C. J. Peters, and T. G. Ksiazek.** 1999. Search for the Ebola virus reservoir in Kikwit, Democratic Republic of the Congo: reflections on a vertebrate collection. J. Infect. Dis. **179**(Suppl. 1):S155–S163.
11. **Maruyama, T., L. L. Rodriguez, P. B. Jahrling, A. Sanchez, A. S. Khan, S. T. Nichol, C. J. Peters, P. W. Parren, and D. W. Burton.** 1999. Ebola virus can be effectively neutralized by antibody produced in natural human infection. J. Virol. **73**:6024–6030.
12. **Miller, R. K., J. Y. Baumgardner, C. W. Armstrong, S. R. Jenkins, C. D. Woolard, G. B. Miller, Jr., L. D. Polk, D. R. Tavris, K. A. Hendricks, J. P. Taylor, D. M. Simpson, S. Schultz, L. Sturman, J. G. Debbie, D. L. Morse, P. E. Rollin, P. B. Jahrling, T. G. Ksiazek, and C. J. Peters.** 1990. Filovirus infections among persons with occupational exposure to nonhuman primates. Morb. Mortal. Wkly. Rep. **39**:266–273.
13. **Miller, R. K., J. Y. Baumgardner, C. W. Armstrong, S. R. Jenkins, C. D. Woolard, G. B. Miller, Jr., P. E. Rollin, P. B. Jahrling, T. G. Ksiazek, and C. J. Peters.** 1990. Filovirus infections in animal handlers. Morb. Mortal. Week. Rep. **39**:221.
14. **Miranda, M. E., T. G. Ksiazek, T. J. Retuya, A. S. Khan, A. Sanchez, C. F. Fulhorst, P. E. Rollin, A. B. Calaor, D. L. Manalo, M. C. Roces, M. M. Dayrit, and C. J. Peters.** 1999. Epidemiology of Ebola (subtype Reston) virus in the Philippines, 1996. J. Infect. Dis. **179**(Suppl. 1):S115–S119.
15. **Niikura, M., T. Ikegami, M. Saijo, I. Kurane, M. E. Miranda, and S. Morikawa.** 2001. Ebola viral antigen-detection enzyme-linked immunosorbent assay using a novel monoclonal antibody to nucleoprotein. J. Clin. Microbiol. **39**:3267–3271.
16. **Peters, C. J., A. Sanchez, P. E. Rollin, T. G. Ksiazek, and F. A. Murphy.** 1996. Filoviridae: Marburg and Ebola viruses, p. 1161–1176. *In* B. N. Fields, D. M. Knipe, and P. M. Howley (ed.), Fields virology, 3rd ed. Lippincott-Raven Publishers, Philadelphia, Pa.
17. **Peters, C. J., and A. S. Khan.** 1999. Filovirus diseases, p. 85–95. *In* H.-D. Klenk (ed.), Marburg and Ebola viruses. Springer-Verlag, Berlin, Germany.
18. **Saijo, M., M. Niikura, S. Morikawa, T. G. Ksiazek, P. F. Meyer, C. J. Peters, and I. Kurane.** 2001. Enzyme-linked immunosorbent assays for detection of antibodies to Ebola and Marburg viruses using recombinant nucleoproteins. J. Clin. Microbiol. **39**:1–7.
19. **Saijo, M., M. Niikura, S. Morikawa, and I. Kurane.** 2001. Immunofluorescence method for detection of Ebola virus immunoglobulin g, using HeLa cells which express recombinant nucleoprotein. J. Clin. Microbiol. **39**:776–778.
20. **Sanchez, A., M. P. Kiley, B. P. Holloway, J. B. McCormick, and D. D. Auperin.** 1989. The nucleoprotein gene of Ebola virus: cloning, sequencing, and in vitro expression. Virology **170**:81–91.
21. **Sanchez, A., T. G. Ksiazek, P. E. Rollin, C. J. Peters, S. T. Nichol, A. S. Khan, and B. W. J. Mahy.** 1995. Reemergence of Ebola virus in Africa. Emerg. Infect. Dis. **1**:96–97.
22. **Sanchez, A., S. G. Trappier, B. J. Mahy, C. J. Peters, and S. T. Nicole.** 1996. The virion glycoproteins of Ebola viruses are encoded in two reading frames and are expressed through transcriptional editing. Proc. Natl. Acd. Sci. USA **93**:3602–3607.
23. **Takada, A., S. Watanabe, K. Okazaki, H. Kida, and Y. Kawaoka.** 2001. Infectivity-enhancing antibodies to Ebola virus glycoprotein. J. Virol. **75**: 2324–2330.
24. **Wilson, J. A., M. Hevey, R. Bakken, S. Guest, M. Bray, A. L. Schmaljohn, and M. K. Hart.** 2000. Epitopes involved in antibody-mediated protection from Ebola virus. Science **287**:1664–1666.
25. **Wilson, J. A., and M. K. Hart.** 2001. Protection from Ebola virus mediated by cytotoxic T lymphocytes specific for the viral nucleoprotein. J. Virol. **75**:2660–2664.
26. **World Health Organization/International Study Team.** 1978. Ebola haemorrhagic fever in Sudan, 1976. Bull. W. H. O. **56**:247–270.
27. **World Health Organization.** 1978. Ebola haemorrhagic fever in Zaire, 1976. Bull. W. H. O. **56**:271–293.
28. **World Health Organization.** 1997. Part one: background information on the organisms and the disease, p. 1–3. *In* W.H.O. recommended guidelines for epidemic preparedness and response: Ebola haemorrhagic fever (EHF). World Health Organization, Geneva, Switzerland.
29. **World Health Organization.** 2001. Outbreak of Ebola haemorrhagic fever, Uganda, August 2000–January 2001. Wkly. Epidemiol. Rec. **76**:41–46.

Available online at www.sciencedirect.com
SCIENCE DIRECT®
Journal of Microbiological Methods 53 (2003) 141–147
Journal of Microbiological Methods
www.elsevier.com/locate/jmicmeth

Review article

Application of the real-time PCR for the detection of airborne microbial pathogens in reference to the anthrax spores

Sou-ichi Makino*, Hyeng-il Cheun

Department of Applied Veterinary Science, Research Center for Animal Hygiene and Food Safety, Obihiro University of Agriculture and Veterinary Medicine, Inada-cho, Obihiro, Hokkaido 080-8555, Japan

Abstract

To establish the rapid detection method of airborne bacterial spores, we examined *Bacillus anthracis* spores by real-time PCR. One hundred liters of air were trapped on a filter of an air monitor device. After it was suspended in PBS, spores of *B. anthracis* were artificially added. The suspension was also heated at 95 °C for 15 min and used for real-time PCR using anthrax-specific primers. A single cell of *B. anthracis* was detected by real-time PCR within 1 h. Our results provide evidence that anthrax spores from the atmosphere can be detected rapidly, suggesting that real-time PCR provides a flexible and powerful tool to prevent epidemics.

Keywords: Real-time PCR; Airborne microorganism; Spore; Anthrax

1. Introduction

Many kinds of microorganisms exist in the air, which are mostly non-pathogenic to humans. However, though it may be artificial or rarely occur, pathogenic microbes sometimes exist in the air and cause respiratory infection. They usually exist in the air as small particles like aerosol, spore or microorganism-binding dust, but most of them will drop on the ground soon because of their own weights. However, they are floating in the air for hours if their diameters are about 1–3 μm and if they are in dried states. Therefore, the spore forming of microorganisms are most suitable for airborne pathogens. Especially, *Bacillus anthrax* is important because of their pathogenicity, meaning that anthrax spores have been assumed as the most effective candidate for the biological weapon for over 80 years and had been used actually in 2001.

Three forms of human anthrax are known: cutaneous, gastrointestinal and pulmonary (inhalation) anthrax. The cutaneous form is often self-limiting, but inhalation anthrax is sometimes severe because antibiotics only suppress the infection if administered shortly after exposure (usually within the first 24–48 h). If not treated by the time the symptoms develop, death is likely to occur in 99% of cases in unprotected individuals (James et al., 1998). Although inhalation anthrax is generally contracted from breathing in airborne anthrax spores, monitoring the exposure of *Bacillus anthracis* spores in the atmosphere is extremely difficult because the spores are not visible to the naked eye, and are colorless, odorless and taste-

* Corresponding author. Tel./fax: +81-155-49-5386.
E-mail address: smakino@obihiro.ac.jp. (S. Makino).

0167-7012/03/$ - see front matter © 2003 Elsevier Science B.V. All rights reserved.
doi:10.1016/S0167-7012(03)00019-8

less. Therefore, a rapid and sensitive technique to detect anthrax spores in the atmosphere is important for public health and probably enough to detect various kinds of airborne microorganism by PCR. In this review, to detect rapidly anthrax spores, we show a PCR detection system using real-time PCR technology.

2. Materials and methods

2.1. Bacterial strains

Nine *B. anthracis* isolates listed in Table 1 (Makino et al., 2001) were used for the PCR. Those strains were inoculated on nutrient agar (NA; Difco Laboratory, Detroit, Mich.) plates and suspended in sterile PBS, followed by preparing their spore suspensions, as previously described (Uchida et al., 1985).

2.2. Isolation of bacterial cells from air samples

One hundred liters of air were trapped on a 0.45-μm nitrocellulose membrane filter using an aerosol analysis monitor (Millipore, Tokyo, Japan), followed by suspending in 1 ml of sterilized PBS or water. As an option, an aliquot of the sample can be inoculated in the appropriate agar plate and broth to detect the organisms, and air-samplers supplied from some companies using NA or blood agar plates are convenient. For *B. anthracis*, blood agar supplemented with polymyxin B, PLET plates (Knisely, 1966) or *Bacillus cereus* selection agar (BCA; Oxoid, Hampshire, England or Merck, Japan) are available.

Table 1
Bacillus strains used in this study

Bacillus strains	PA	CAP
Shikan	+	+
Morioka	−	+
Pasteur II	+	+
Pasteur I	+	+
Nakagawa	−	+
Ryugasaki	+	+
52	+	+
P-I	+	+
34-F2	+	−

2.3. Preparation of DNA samples for PCR

The suspension is centrifuged at 15,000 rpm for 5 min and resuspended in 10 μl of sterile water, followed by heating at 95–100 °C for 15 min and centrifugation at 15,000 rpm for few minutes at 4 °C, and then 1 μl of the supernatant was directly used for PCR. Since spores might be contained in the samples, a class IIb safety cabinet should be used for the preparation.

2.4. PCR

Oligonucleotide primers for PCR were as follows: specific primers (CAP primers) to amplify a 591-bp DNA fragment of the *cap* region essential for encapsulation (Makino et al., 1989), MO11 (5′-GACGGATTATGGTGCTAAG-3′) and MO12 (5′-GCACTGGCAACTGGTTTTG-3′); specific primers (PA primers) to amplify a 211-bp fragment of the *pag* gene to produce a component of the toxin (Price et al., 1999), PA7 (5′-ATCACCAGAGGCAAGACACCC-3′) and PA6 (5′-ACCAATATCAAAGAACGACGC-3′). For standard PCR, all primers, 20 pmol each, were mixed in a reaction tube, and PCR was performed in a reaction mixture (25 μl) using model 9600 (Applied Biosystems Japan, Tokyo, Japan). The following PCR cycles were used: 1 × 95 °C for 2 min; 35 × (95 °C for 15 s followed by 60 °C for 15 s followed by 72 °C for 30 s); 1 × 72 °C for 5 min; cool to 4 °C. The real-time PCR was performed using two systems of Light Cycler (Roche Diagnostic, Tokyo Japan) and Smart Cycler (Takara shuzo, Kyoto Japan), which was originally from Cepheid, CA, USA. PCR amplification was performed according to the supplier's instructions. For the Light Cycler system, Light Cycler™ FastStart DNA Master SYBR Green I (Roche Diagnostic) was used. For the Smart Cycler system, TaKaRa *B. anthracis* PCR Detection Kit (Real-Time PCR Version) (Takara shuzo) was used, which consisted of each primer set as described above and internal control to prevent false positive; in the negative reaction, 152 and 395 bp PCR products with 80 and 82 °C melting peaks using CAP and PA primers, respectively. The following PCR cycles were used: 1 × 95 °C for 10 min; 40 × (95 °C for 10 s followed by 64 °C for 10 s followed by 72 °C for 20 s) for the Light Cycler and 1 × 95 °C for 30 s;

40 × (95 °C for 5 s followed by 68 °C for 30 s) for the Smart Cycler.

3. Results and discussion

3.1. Standard PCR Technology

Generally, 10–1000 bacterial cells in the suspension prepared from 100 l of air should be detected on the NA plates. When anthrax spores were artificially contaminated into such suspensions followed by spreading on the BCA plates, background bacterial cells grew, but large rough colonies of *B. anthracis* cells were detected on the plates (Fig.1). These rough colonies were subsequently confirmed by PCR.

Standard PCR with two sets of primers was performed using the DNA samples prepared, showing that those primers amplified the right sizes of two DNA fragments using DNA samples containing over 10 spores, but that the DNA fragments detected were faint using DNA samples containing only one spore (Fig. 2, panel A, lane 2).

3.2. Light Cycler

The conditions for real-time PCR using Light Cycler were found using DNA samples prepared as in the standard PCR and CAP primers. The highest annealing temperature was the temperature at which no amplified fragment was detected using a sample with no spores. Thus, the PCR cycle for the Light Cycler system was determined as described in Materials and methods (Fig. 3, panel A). Simultaneously, the fluorescence signals were measured using the quantification program of Light Cycler software version 4.2 (Roche Diagnostics). As the copy number of the *cap* gene correlates with numbers of spores, the relative numbers of spores in the samples should be estimated by measuring the fluorescence signals. When the copy numbers of the *cap* gene in the samples containing one spore was one, the relative copy number of the *cap* gene in the samples containing 10 and 100 spores were estimated as 9.95 and 100.02, respectively. Thus, when samples containing known numbers of cells were used as standards in real-time PCR, the number of spores in a sample can be estimated.

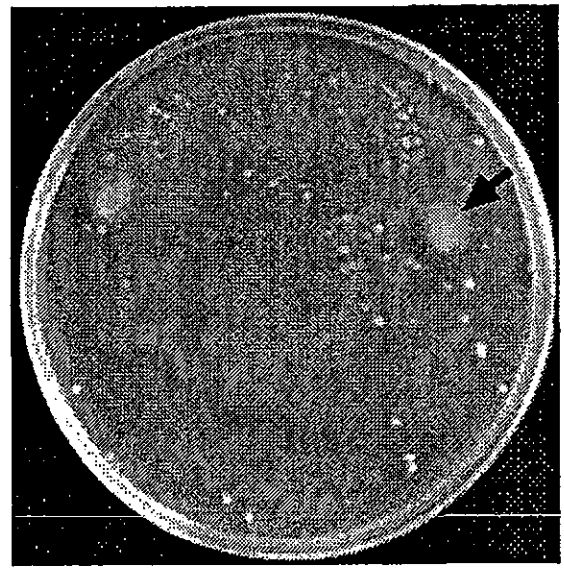

Fig. 1. Isolation of anthrax spores on a BCA plate. The suspension from 100-l air sample containing one spore was plated on a BCA plate. The arrow shows a colony of *B. anthracis*.

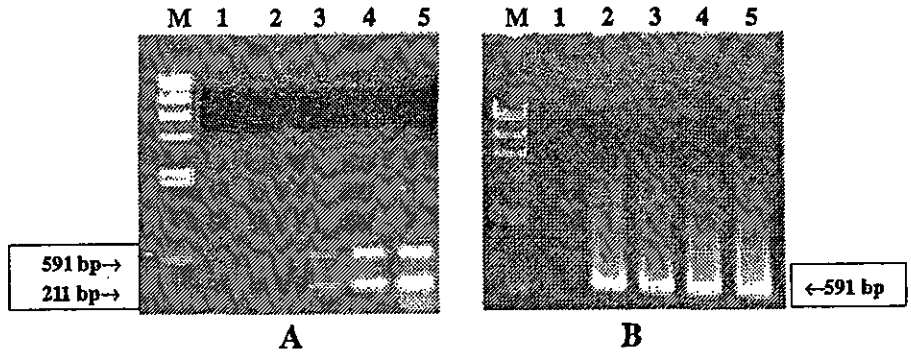

Fig. 2. Detection of anthrax DNA from air samples using PCR. Template DNAs were prepared from air samples containing 0 (lane 1), 1 (lane 2), 10 (lane 3) and 100 (lane 4) anthrax spores, and then were used for standard PCR (A) and real-time PCR (B). M, λ DNA digested with HindIII as the molecular size marker; lane 5, purified DNA.

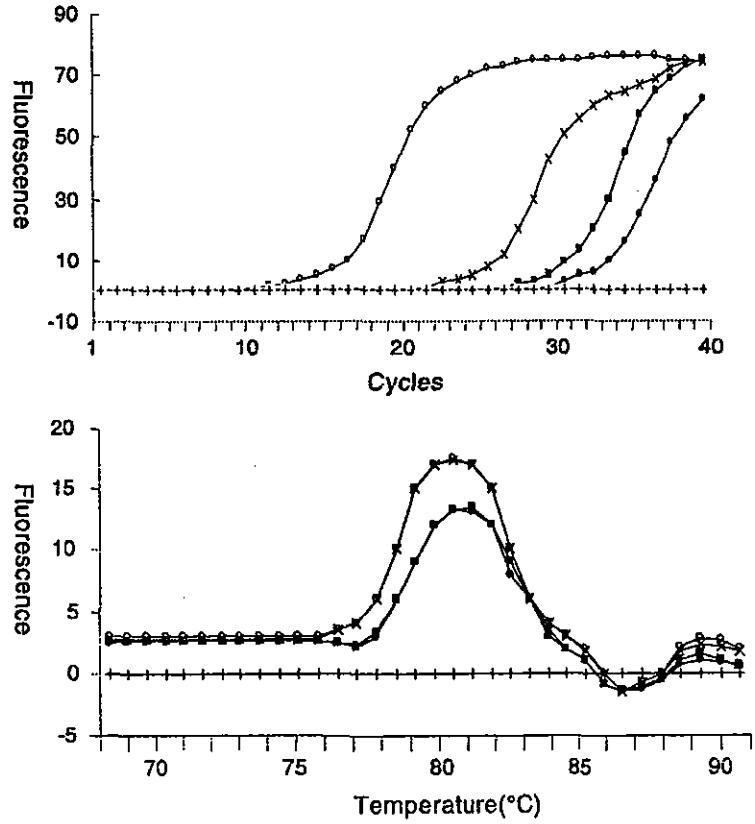

Fig. 3. Fluorescence graph (A) and melting curve (B) using the Light Cycler system. O—purified DNA; × —100 spores per sample; ■—10 spores per sample; ●—1 spore per sample; ÷—0 spore per sample.

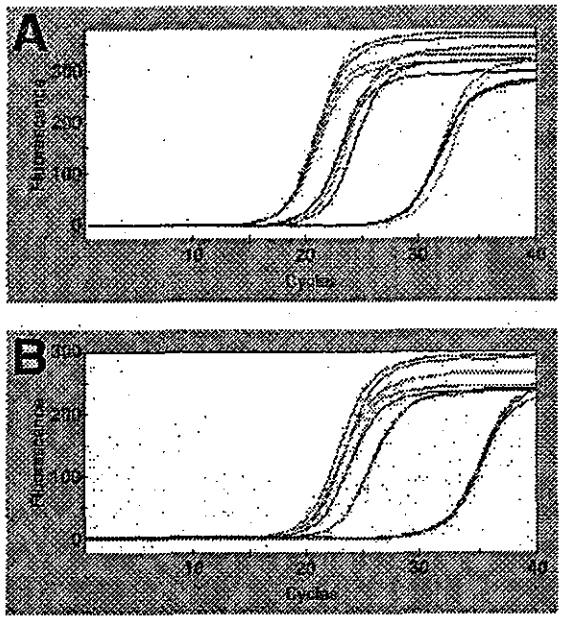

Fig. 4. Fluorescence graphs using PA (A) and CAP (B) primers in the Smart Cycler system. Internal control was always amplified after 30 cycles in negative samples.

To analyze the melting curve, the PCR products was set up with a target temperature of 95 °C using Light Cycler software version 4.2, which was performed immediately after the amplification finished. This program can differentiate between signals obtained from specific PCR products and nonspecific DNA fragments, such as primer-dimer, and thus, specific PCR products must show the same melting peaks. In this study, the melting peaks of the amplified products were about 84.5 °C (Fig. 3, panel B), showing that we could recognize amplified specific products without electrophoresis. To confirm that PCR was successful, the amplified products were electrophoresed in agarose gel. Specific PCR products were detected, even in the sample containing one spore (Fig. 2, panel B). The same PCR conditions and results were obtained using PA primers except with a melting peak of about 82 °C (data not shown).

3.3. Smart Cycler

The real-time PCR with Smart Cycler was performed using airborne samples, which were artificially contaminated with each 100 spores from nine strains, by a new PCR kit, and then the fluorescence signals were measured using those samples. The signals were detected at about 20 cycles in positive samples, but the signals, which were generated from the internal control, were detected at about 30 cycles in negative samples (Fig. 4).

To analyze the melting curve, the PCR products was set up with a target temperature of 95 °C. In this study, the melting peaks of the amplified products using PA primers were about 82 °C in positive samples and about 80 °C in negative samples (Fig. 5, panel A). The peaks using MO primers were about 85 °C in positive samples and about 82 °C in negative samples (Fig. 5, panel B), showing that we could recognize amplified specific products without electrophoresis. To confirm that PCR was successful, the amplified products were electrophoresed in agarose gel. Specific PCR products of 211 and 152 bp in positive and negative samples, respectively, were detected using PA primers (Fig. 6. panel A), and also positive 591 bp and negative 395 bp DNA fragments were detected using CAP primers (Fig. 6, panel B).

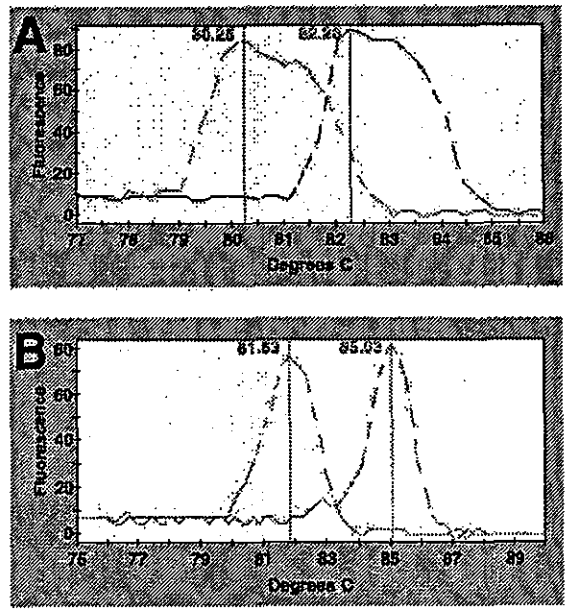

Fig. 5. Melting curves using PA (A) and CAP (B) primers in the Smart Cycler system. Melting peaks of the PCR products amplified by PA and CAP primers were about 82 and 85 °C, respectively. Lower peaks were derived from the PCR products amplified by the internal control.

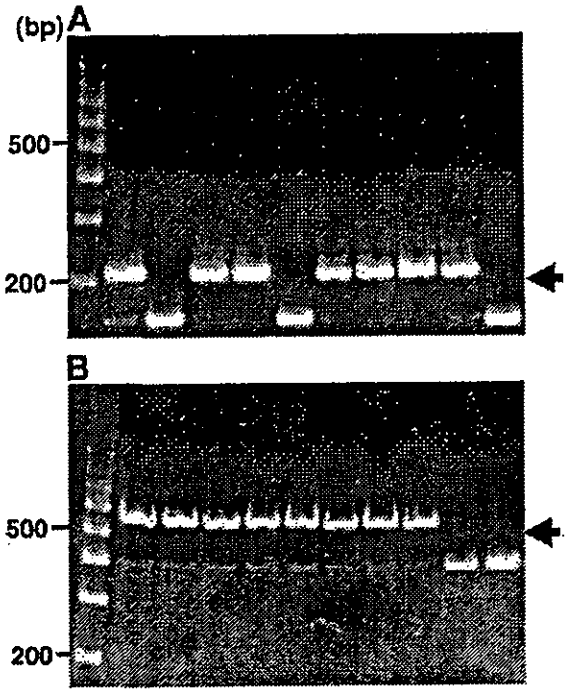

Fig. 6. Detection of anthrax DNA from air samples using the Smart Cycler system. Template DNAs were prepared from air samples containing about 100 anthrax spores of Shikan (lane 1), Morioka (lane 2), Pasteur II (lane 3), Pasteur I (lane 4), Nakagawa (lane 5), Ryugasaki (lane 6), 52 (lane 7), P-I (lane 8) and 34-F2 (lane 9) using PA (A) and CAP (B) primers. M, 100 bp DNA ladder; lane 10, without spores. The arrow shows PCR product in the positive sample. Shorter products were amplified by the internal control in the negative sample.

We showed that template DNA for PCR could be prepared from air samples within 1 h by heating. We also purified template DNA using a DNA extraction kit (Qiagen K.K. Japan, Tokyo) with the results of PCR identical to those by heating, but preparing template DNA using this kit took about 2 h. From the results, heat treatment alone proved sufficient to prepare template DNA for PCR and had the advantage of a shorter time than using the kit.

Target fragments were detected within 4 h using the standard PCR system, and within 1 h using the real-time PCR system, which also had the advantage of making it possible to estimate the number of anthrax spores in the air and to confirm the amplification of target products using only melting curve analysis without agarose gel electrophoresis. In addition, the PCR kit used in this study might be more convenient because of an internal control. Generally, detecting *B. anthracis* infection and diagnosing anthrax in humans is difficult because early symptoms are nonspecific. However, monitoring anthrax spores in the environment, especially in the air, can aid detection and prevent *B. anthracis* infections in humans. This real-time PCR system using the Light Cycler is a flexible and powerful tool to prevent epidemics because it can detect one spore in an air sample. Also, this real-time PCR system can detect *B. anthracis* cells from food, drink and soil, which are thought to be other sources of anthrax. However, preparation of template DNA for PCR would be more difficult from these other sources than from air samples because of the large number of cells of various bacterial species, organic compounds, etc. (manuscript in preparation).

In this study, we showed that one *B. anthracis* spore in 100 l of air sample can be detected using PCR and we also showed the isolation of one spore on a

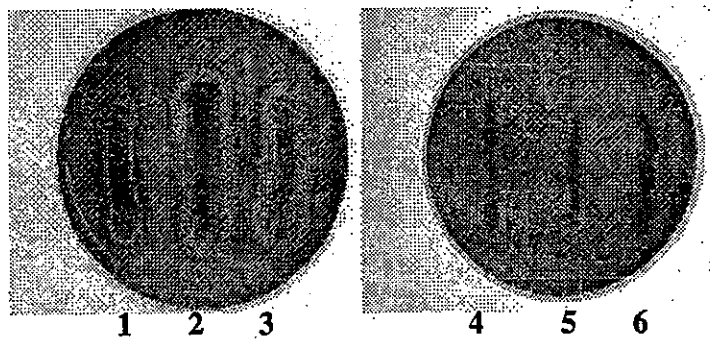

Fig. 7. Haemolysis on blood agar plates of *Bacillus* strains. *B. cereus* (1), *B. mycoides* (2), *B. thuringiensis* (3) and *B. anthracis* (4–6) strains were streaked on blood agar plates supplemented with the BCA supplement. Those plates were incubated at 37 °C for 16 h.

BCA plate. As we can isolate *B. anthracis* vegetative cells from meat and tissue effectively using BCA plates (Cheun et al., 2001), a BCA plate would be a effective tool to detect *B. anthracis* from various samples. At the same time, blood agar plates supplemented with the same supplement used with BCA were also effective because hemolysis was easily detected (Fig. 7). Finally, for the initial examination, real-time PCR and direct plating onto selection plates would have to be done at the same time. If the samples contain more than one spore, the PCR method can detect the existence of *B. anthracis* spores in the air within 1 h and can isolate *B. anthracis* cells within 2 days. Such an automatic monitoring system for *B. anthracis* might be an essential tool for epidemiological surveys and for the prevention of *B. anthracis* infections in the future. In this article, we showed the application of the real-time PCR only in anthrax spores, but this procedure should be available to detect rapidly other airborne microorganisms.

Acknowledgements

This work was supported in part by grants from the Ministry of Health, Labour and Welfare (Research on Emerging and Re-emerging Infectious Diseases), by a Grant-in Aid for Scientific Research from the Japanese Society for the Promotion of Science (12575029), and by a grant from "The 21st Century COE Program (A-1)", Ministry of Education, Culture, Sports, Science and Technology, Japan.

References

Cheun, H.I., Makino, S.-I., Watarai, M., Shirahata, T., Uchida, I., Takeshi, K., 2001. A simple and sensitive detection system of *Bacillus anthracis* in meat and tissue. J. Appl. Microbiol. 91, 421–426.

James, C.P., John, D.M., Edward, M.E., Arthur, M.F., 1998. Anthrax as a potential biological warfare agent. Arch. Intern. Med. 158, 429–434.

Knisely, R.F., 1966. Selective medium for *Bacillus anthracis*. J. Bacteriol. 92, 784–786.

Makino, S.-I., Uchida, I., Terakado, N., Sasakawa, C., Yoshikawa, M., 1989. Molecular characterization and protein analysis of the cap region, which is essential for encapsulation in *Bacillus anthracis*. J. Bacteriol. 171, 722–730.

Makino, S.-I., Cheun, H.I., Watarai, M., Uchida, I., Takeshi, K., 2001. Detection of anthrax spores from the air using real-time PCR. Lett. Appl. Microbiol. 33, 1–4.

Price, L.B., Hugh-Jones, M., Jackson, P.J., Keim, P., 1999. Genetic diversity in the protective antigen gene of *Bacillus anthracis*. J. Bacteriol. 181, 2358–2362.

Uchida, I., Sekizaki, T., Hashimoto, K., Terakado, N., 1985. Association of the encapsulation of *Bacillus anthracis* with a 60 megadalton plasmid. J. Gen. Microbiol. 131, 363–367.

INFECTION AND IMMUNITY, June 2003, p. 3020–3027 Vol. 71, No. 6
0019-9567/03/$08.00+0 DOI: 10.1128/IAI.71.6.3020–3027.2003

Isolation and Characterization of Mini-Tn5Km2 Insertion Mutants of *Brucella abortus* Deficient in Internalization and Intracellular Growth in HeLa Cells

Suk Kim, Masahisa Watarai,* Yuki Kondo, Janchivdorj Erdenebaatar, Sou-ichi Makino, and Toshikazu Shirahata

Department of Applied Veterinary Science, Obihiro University of Agriculture and Veterinary Medicine, Obihiro, Hokkaido 080-8555, Japan

Received 9 January 2003/Returned for modification 11 February 2003/Accepted 28 February 2003

***Brucella* spp. are facultative intracellular pathogens that have the ability to survive and multiply in professional and nonprofessional phagocytes and cause abortion in domestic animals and undulant fever in humans. The mechanism and factors of virulence are not fully understood. To identify genes related to internalization and multiplication in host cells, *Brucella abortus* was mutagenized by mini-Tn5Km2 transposon that carryied the kanamycin resistance gene, 4,400 mutants were screened, and HeLa cells were infected with each mutant. Twenty-three intracellular-growth-defective mutants were screened and were characterized for internalization and intracellular growth. From these results, we divided the mutants into the following three groups: class I, no internalization and intracellular growth within HeLa cells; class II, an internalization similar to that of the wild type but with no intracellular growth; and class III, internalization twice as high as the wild type but with no intracellular growth. Sequence analysis of DNA flanking the site of transposon showed various insertion sites of bacterial genes that are virulence-associated genes, including *virB* genes, an ion transporter system, and biosynthesis- and metabolism-associated genes. These internalization and intracellular-growth-defective mutants in HeLa cells also showed defective intracellular growth in macrophages. These results suggest that the virulence-associated genes isolated here contributed to the intracellular growth of both nonprofessional and professional phagocytes.**

Brucellosis is a major bacterial zoonosis that causes a serious debilitating disease in humans and abortion and sterility in domestic animals. The etiologic agents of brucellosis are *Brucella* spp., small gram-negative and facultative intracellular pathogens that can multiply within professional and nonprofessional phagocytes (9, 10). In contrast to other intracellular pathogens, *Brucella* species do not produce exotoxins, antiphagocytic capsules or thick cell walls, resistance forms, or fimbriae and do not show antigenic variation (16). A key aspect of the virulence of brucella is its ability to proliferate within professional and nonprofessional phagocytic host cells and thereby successfully bypasses the bactericidal effects of phagocytes, and their virulence and chronic infections are thought to be due to their ability to avoid the killing mechanisms within host cells (30, 41). The molecular mechanisms and genetic basis for intracellular survival and replication, however, are not understood completely. Some studies with nonprofessional phagocytes have shown that *Brucella* invades host cells and is contained within early endosome-like vacuoles. These vacuoles rapidly fuse with early autophagosomes that acquire vacuolar [H^+]ATPase and lysosome-associated membrane proteins (LAMP), mature into a late autophagosome, inhibit fusion with lysosomes, and finally become a replicating vacuole normally associated with the endoplasmic reticulum (5, 11, 31, 32). The genetic basis of *Brucella* virulence is still poorly understood. The VirB type IV secretion system of *Brucella* has been identified recently (29). This operon is composed of 13 open reading frames (ORFs) that share homology with other bacterial type IV secretion systems in the intracellular trafficking of pathogens. Deletion or polar and nonpolar mutations of these ORFs were not able to replicate and survive within phagocytes (39, 44). Thus, the VirB proteins of *B. abortus* are thought to be constituents of the secretion apparatus.

To identify bacterial virulence genes, transposon mutagenesis is the most frequently used approach as a genetic tool (19). Various mini-Tn5 derivatives carrying standard selectable antibiotic resistance markers have been described for genetic analysis (6). Transposon insertion in any *Brucella* gene concerned with intracellular survival and replication may reduce the virulence of *Brucella* in phagocytes or experimental animals, and the identification of *Brucella* virulence associated genes may be easier.

We identified here several genes that encode factors required for the internalization and intracellular growth of *B. abortus* within professional and nonprofessional phagocytes by using mini-Tn5Km2 transposon, and we examined their characteristics. The virulence of mutants was evaluated by infecting mice with transposon mutants. Possible roles in the virulence of *Brucella* for the different factors identified are discussed.

MATERIALS AND METHODS

Bacterial culture and media. All *B. abortus* derivatives were from 544 (ATCC 23448), smooth virulent *B. abortus* biovar 1 strains. *B. abortus* strains were maintained as frozen glycerol stocks and were cultured in brucella broth (Becton Dickinson, Sparks, Md.) or brucella broth containing 1.5% agar. Kanamycin (30

* Corresponding author. Mailing address: Department of Applied Veterinary Science, Obihiro University of Agriculture and Veterinary Medicine, Inada-cho, Obihiro-shi, Hokkaido 080-8555, Japan. Phone: 81-155-49-5387. Fax: 81-155-49-5386. E-mail: watarai@obihiro.ac.jp.

μg/ml) and nalidixic acid (25 μg/ml) were used when necessary. *Escherichia coli* DH5α and *E. coli* S-17λ*pir* pUT mini-Tn*5*Km2 were used for transformation and transposon conjugation, respectively (17, 40). Each *E. coli* was cultured in Luria-Bertani broth or agar. If necessary, ampicillin (100 μg/ml) and kanamycin (30 μg/ml) were used. Bacterial growth rates were measured spectrophotometrically at 600 nm.

A modified version of the antibiotic agar dilution method of the National Committee for Clinical Laboratory Standards was used for determination of MIC for gentamicin (35). The MIC was defined as the lowest concentration of the antibiotic tested giving complete inhibition of bacterial growth compared with drug-free control.

Cell culture. HeLa cells were grown at 37°C in a 5% CO_2 atmosphere in Eagle minimum essential medium (MEM; Sigma, St. Louis, Mo.) containing 10% fetal bovine serum (FBS). Bone marrow-derived macrophages from female BALB/c mice were prepared by the method described previously (42). After culture in L-cell conditioned medium, the macrophages were replated for use by lifting cells in phosphate-buffered saline (PBS) on ice for 5 to 10 min, harvesting by centrifugation, and resuspension in RPMI 1640 (Sigma) containing 10% FBS. The HeLa cells or macrophages were seeded (2×10^5 to 3×10^5 per well) in 24-well tissue culture plates 1 day before infection for all assays.

Construction of mini-Tn*5*Km2 mutants. To obtain a selectable marker for conjugation, mini-Tn*5*Km2 transposon (6) carrying the kanamycin resistance gene was introduced into pUT, a transposon donor vector, to form pUT mini-Tn*5*Km2. The mini-Tn*5*Km2-bearing plasmid pUT mini-Tn*5*Km2 was introduced into *B. abortus* from an *E. coli* K-12 derivative, SM17λ*pir* (7), by conjugation, and transposon mutagenesis of *B. abortus* by conjugation was done as described previously (17, 27). The mutants thus obtained were purified on agar plates containing kanamycin (30 μg/ml) and were screened intracellular growth defective mutants within HeLa cells, and the mutants were kept in 20% glycerol in brucella broth at −80°C.

Infection and intracellular survival assay. Bacterial infection and intracellular survival assay was done by using the modified method described previously (43). Briefly, *B. abortus* mutants were deposited onto HeLa cells grown on 96-well microtiter plates filled with MEM plus 10% FBS at a multiplicity of infection of 20, centrifuged at 150 × *g* for 10 min at room temperature, incubated at 37°C in 5% CO_2 for 1 h, washed twice with 0.5 ml of sterile PBS, and incubated with MEM plus gentamicin (30 μg/ml) for 48 h. After incubation, the cells were washed and lysed with 0.1 ml of sterile distilled water, and 25 μl of the sample was dropped onto brucella agar and was incubated at 37°C for 48 h. After incubation, no growth samples on brucella agar were considered intracellular-growth-defective mutants and were selected. This assay was done at least three times.

DNA sequencing. The DNA was sequenced by the following standard techniques (37). Chromosomal DNA of the mutants was digested with *Eco*RI, cloned to plasmid pBluescript II KS(+) (Toyobo, Tokyo, Japan), transformed into *E. coli* DH5α, and plated onto Luria-Bertani agar containing ampicillin (100 μg/ml) and kanamycin (30 μg/ml). Plasmid DNA was extracted by using the plasmid Mini Kit (Qiagen), and the chromosomal DNA sequence was analyzed by using the mini-Tn*5*Km2 transposon O′-end primer (5′-CCTCTAGAGTCGACCTGC AG-3′). The chromosomal DNA sequence database was searched by using BLASTX and BLASTN search algorithms (http://www.genome.ad.jp/and http://www.ncbi.nml.nih.gov/blast/).

Southern blot analysis. After chromosomal DNA was extracted, it was digested for 2 h with *Bam*HI restriction enzymes (none of which digest a DNA-specific probe for mini-Tn*5*Km2), separated by electrophoresis in 0.8% agarose, and transferred to positively charged nylon membranes. A 1.7-kb *Eco*RI and *Xba*I fragment that contained the kanamycin resistance gene of mini-Tn*5*Km2 was labeled by using a biotin nonisotopic labeling kit, and it was used as the DNA probe for Southern hybridization under stringent conditions.

Determination of efficiency of bacterial uptake and intracellular growth by cultured HeLa cells and macrophages. To determine the uptake of bacteria and intracellular growth, HeLa cells and mouse bone marrow-derived macrophages were infected with *B. abortus* as described above. For analysis of bacterial uptake efficiency, both types of cells were washed once with medium after 0, 5, 15, 25, and 35 min of incubation at 37°C and then incubated with MEM or RPMI 1640 with gentamicin (30 μg/ml) for 30 min. Both types of cells were then washed three times with PBS and then lysed with distilled water. CFU were measured by serial dilutions on brucella plates. For intracellular growth efficiency, both infected cells were incubated at 37°C for 30 min, washed once with medium, incubated with MEM or RPMI 1640 plus gentamicin (30 μg/ml), and then incubated for 2, 24, and 48 h. Cell washing, lysis, and plating procedures were the same as for the analysis of the efficiency of bacterial uptake. The percent protection was calculated by dividing the number of bacteria surviving the assay by the number of bacteria in the infectious inoculum, as determined by viable counts.

LAMP-1 staining. LAMP-1 staining was performed by using the method described previously (43). Briefly, infected macrophages were fixed in 4% periodate-lysine-paraformaldehyde-sucrose for 1 h at 37°C. All antibody-probing steps were for 1 h at 37°C. Samples were washed three times in PBS for 5 min and then permeabilized at −20°C in methanol for 10 s. After three 5-min incubations with a blocking buffer (2% goat serum in PBS), the samples were stained with anti-LAMP-1 rat monoclonal antibody 1D4B diluted 1:100 in blocking buffer. After three washes for 5 min in blocking buffer, the samples were stained with Texas red-goat anti-rat immunoglobulin G. The samples were stained with anti-*B. abortus* polyclonal rabbit serum and fluorescein isothiocyanate-conjugated goat anti-rabbit immunoglobulin G in blocking buffer to identify the bacteria, placed in mounting medium, and then visualized by fluorescence microscopy. One hundred bacteria within macrophages were selected randomly, and the extent of LAMP-1 acquisition of bacteria was determined.

Bacterial adherence assay. Bacterial adherence was assayed by a previously described method (45). Briefly, before bacterial infection HeLa cells were incubated with MEM containing cytochalasin D (500 μg/ml) for 40 min at 37°C, and bacterial infection, fixation, staining, and microscopic evaluation were done as described above for bacterial detection. One hundred HeLa cells were selected randomly, and the adherent bacteria on cells were counted.

Labeling bacterial surface proteins. To examine the modification of bacterial surface proteins, 1-ml samples of cultured bacteria were harvested by centrifugation, washed twice with PBS, and suspended in 200 μl of PBS. Then, 10 μl of 1% of Sulfo-NHS-Biotin (Pierce, Rockford, Ill.) was added, and the mixture was placed on ice for 2 min. NHS ester reacts with the deprotonated form of the primary amine. After one wash with PBS, each sample (40 μg) was mixed with sodium dodecyl sulfate sample buffer, incubated at 100°C for 5 min before loading, and subjected to sodium dodecyl sulfate-polyacrylamide gel electrophoresis. The proteins were electrotransferred to nitrocellulose membranes and were incubated with horseradish peroxidase-conjugated streptavidin. The blot was developed with Western blot detection reagents (Amersham Pharmacia Biotec).

Virulence in mice. The virulence was determined by quantifying the survival of the strains in the spleen after 10 days. Six-week-old female BALB/c mice were infected intraperitoneally with ca. 10^4 CFU of brucellae in 0.1 ml of saline. Groups of five mice were infected with each strain. At 10 days postinfection the mice were sacrificed by decapitation, and their spleens were removed, weighed, and homogenized in saline. Tissue homogenates were serially diluted with PBS and were plated on brucella agar to count the number of CFU in each spleen.

RESULTS

Isolation of intracellular-growth-defective mutants. To identify intracellular-growth-defective mutants within HeLa cells, we randomly mutagenized *B. abortus* with the mini-Tn*5*Km2 transposon, and mutants were selected on brucella plates containing antibiotics. Nonmutagenized bacteria did not grow, but mutants carrying the transposon inserted in the chromosome were resistant to antibiotics. From this result, 4,400 mutants were screened, and HeLa cells were infected with each mutant, and then intracellular-growth-defective mutants were screened (see Materials and Methods); 23 of the mutants did not survive within HeLa cells (Table 1). To confirm how many of each clone contained the transposon insertion site and whether mutants contain the transposon in chromosomal DNA, the chromosomal DNA of all mutants was extracted, digested with *Bam*HI (no site in the transposon), and then hybridized by Southern blot analysis with a mini-Tn*5*Km2 probe; all mutants contained a single transposon in chromosomal DNA (data not shown).

Characterization of mutants. To investigate whether internalization into host cells of *B. abortus* contributes to intracellular growth, HeLa cells were infected with each mutant, and the ability of bacterial internalization was assessed. Of the 23 insertion mutants 2, K18 and K41, lost their ability to internal-

TABLE 1. *B. abortus* genes essential for intracellular growth

Functional group and mutant	Class	Mutated genes (putative functions)	*B. melitensis* ORF[a]	*B. suis* ORF[b]
Transport				
K2	III	*znuA* (zinc uptake system)	II0178	II1122
K13	III	*virB3* (type IV secretion system)	II0027	II0067
K26	III	*virB5* (type IV secretion system)	II0029	II0065
K40	III	*virB4* (type IV secretion system)	II0028	II0066
K46	III	*virB5* (type IV secretion system)	II0029	II0065
K50	III	*virB5* (type IV secretion system)	II0029	II0065
K51	III	*virB6* (type IV secretion system)	II0030	II0064
K52	III	*virB6* (type IV secretion system)	II0030	II0064
K55	III	*virB6* (type IV secretion system)	II0030	II0064
Amino acid synthesis, K17	III	*aspC* (aminotransferase)	I0516	I1495
Sugar metabolism				
K15	II	*zwf* (pentose phosphate pathway)	II0513	II0778
K18	I	*gnd* (pentose phosphate pathway)	II1124	II0111
DNA/RNA metabolism				
K6	III	*purM* (purines)	I1240	I0710
K9	III	*purL* (purines)	I1127	I0837
K11	III	*pyrB* (pyrimidines)	II0670	II0599
K19	II	*purN* (purines)	I1241	I0709
K45	III	*pyrC* (dihydroorotase)	II0669	II0600
K63	III	*pyrC* (dihydroorotase)	I1281	I0668
W27	II	*pth* (peptidyl tRNA hydrolase)	I0480	I1536
Regulation, K41	I	*spoT* (stringent response)	I1296	I0652
Oxidoreduction, K54	III	*cydC* (cytochrome oxidase)	II0761	II0508
Membrane structure, K23	III	*dacF* (peptidoglycan synthesis)	II0350	II0947
Nicotinamide metabolism, K48	II	*pncA* (pyrazinamidase)	I0545	I1417

[a] ORF of *B. melitensis* genome on the NCBI Entrez Genome website (http://www.ncbi.nlm.nih.gov/PMGifs/Genomes/micr.html).
[b] ORF of *B. suis* genome on the NCBI Entrez Genome website (http://www.ncbi.nlm.nih.gov/PMGifs/Genomes/micr.html).

ize almost completely, and these mutants were classified as class I strains. Four mutants—K15, K19, K48, and W27—showed the same ability to internalize as the wild-type strain, and they were classified as class II strains. The other 17 mutants showed an ability to internalize that was twice as high as the wild-type strain, and they were classified as class III (Table 1). Figure 1A and 2A show typical results of using one mutant in each class at various times of incubation. To eliminate the possibility that these results were caused by a change in sensitivity to gentamicin, the sensitivity of these mutants to gentamicin was tested. The wild-type strain and each mutant showed identical sensitivities to gentamicin.

The intracellular survival of *Brucella* spp. has been documented for several cell types. *B. abortus* shows a different intracellular trafficking pattern between professional and nonprofessional phagocytes (1, 11, 30). To analyze whether virulence-associated genes isolated in the present study share intracellular growth between professional and nonprofessional phagocytes, bone marrow-derived macrophages were infected with each mutant, and its internalization and intracellular growth within macrophages was examined. The results of the internalization and intracellular growth of mutants were compared to those with the wild-type strain. All class I strains, two class II strains (K15 and K19), and three class III strains (K6, K9, and K11) showed a three-fold-lower ability to internalize than the wild type and no intracellular growth within macrophages. The other 2 class II strains and 14 class III strains showed an ability to internalize similar to the wild type and no intracellular growth within macrophages. Figure 1B and 2B show typical results of using one mutant in each class after various incubation times.

Phagosomes containing virulent *B. abortus* are reluctant to fuse with lysosomes, whereas dead *B. abortus* phagosomes colocalize with endocytic compartments in the early stage of infection in macrophages (1). To test the ability of *B. abortus* to target properly within macrophages early in infection, interaction of the mutants with the endocytic pathway was quantified by immunofluorescence localization of LAMP-1, a membrane protein of late endosomes and lysosomes (3, 21). As expected, most phagosomes containing the wild-type strain did not colocalize with LAMP-1 (12.3% ± 3.4% positive). In contrast, phagosomes containing a mutant in each class were frequently stained brightly by LAMP-1 antibody at 30 min of incubation (Fig. 3). This finding suggests that, in contrast to the wild-type strain, these mutants are colocalizing with either late endosomes or lysosomes.

To investigate whether adherence of the mutants to HeLa cells contributes to bacterial internalization ability, the initial adherence of the mutants to HeLa cells was analyzed. Class II and III strains showed an adhesion ability twice as high as that of the wild-type strain and class I strains. Figure 4 shows typical results of using one mutant in each class after various incuba-